JOURNAL OF CATALYSIS **129,** 38–46 (1991)

Acidic Properties of Oxides Containing Niobia on Silica and Niobia in Silica

P. A. BURKE[1] AND E. I. KO[2]

Department of Chemical Engineering, Carnegie Mellon University, Pittsburgh, Pennsylvania 15213

Received August 20, 1990; revised December 10, 1990

A series of composite oxides containing niobia (Nb_2O_5) and silica (SiO_2) was prepared by either incipient wetness impregnation to form surface phase oxides or by coprecipitation to form mixed oxides. At low Nb_2O_5 concentrations, both the surface phase and mixed oxides showed strong Lewis acidity as determined by thermogravimetric and infrared studies of adsorbed pyridine. A surface phase oxide containing 0.25 monolayer of Nb_2O_5 on SiO_2 further showed strong Brønsted acidity. With increasing Nb_2O_5 concentration and/or treatment temperature, Nb_2O_5 in these composite oxides became more bulk-like and showed a corresponding decrease in acid strength. These acidic properties are discussed in terms of proposed structural models which contain tetrahedral niobia, octahedral niobia, and Nb=O bonds as basic building blocks.

INTRODUCTION

It is well known that the combination of two oxides often leads to interesting acidic properties. Both Tanabe (*1*) and Kung (*2*) have proposed models to predict the formation of acid sites when two oxides are combined to form a mixed oxide. More recently, Dumesic and co-workers (*3, 4*) have discussed the generation of acid sites when one oxide is deposited onto another to form a surface phase oxide. Although mixed and surface phase oxides appear to be different systems at first glance, the origins of acidity in them really share a fundamental basis of how the two oxides interact with each other.

In our work with using niobia (Nb_2O_5) to modify the support behavior of silica (SiO_2), we have found that the way by which the two oxides are brought together affects the ensuing metal-support interactions with nickel (*5*). With respect to hydrogen chemisorption and CO hydrogenation, Nb_2O_5 on SiO_2 as a support behaves similarly to Nb_2O_5 but Nb_2O_5 in SiO_2 does not. These results suggest that although Nb_2O_5 is interacting with SiO_2 in both the surface phase and mixed oxides, the nature of interactions seems to be different. It is thus of interest to ascertain whether Nb_2O_5–SiO_2 interactions lead to acidity in these composite oxides and to identify any differences in their acidic properties.

Niobia in its hydrated form is known as niobic acid, a catalyst active for isomerization and dehydration (*6*). However, its acidity diminishes with increasing calcination temperature and becomes negligible after a pretreatment at 773 K (*7*). When Nb_2O_5 is grafted onto SiO_2, Iwasawa and co-workers have found that the resulting catalyst is active for the dehydrogenation and dehydration of ethanol (*8, 9*) and possesses both Lewis and Brønsted acid sites (*10*). Datka *et al.* (*11*) recently reported that the deposit of Nb_2O_5 onto supports such as SiO_2, Al_2O_3, TiO_2, ZrO_2, and MgO also introduces acid sites. The distribution of Lewis and Brønsted acid sites depends on the support and the loading of Nb_2O_5. Okazaki and Okuyama (*12*) showed that Nb_2O_5/TiO_2 mixed oxides, prepared from coprecipitation, are

[1] Present address: IBM, B31/972-1, Essex Junction, VT 05452.

[2] To whom correspondence should be addressed.

0021-9517/91 $3.00

acidic and active in the reduction of NO with NH_3. To our knowledge the acidic behavior of Nb_2O_5/SiO_2 mixed oxides has not been established.

In this study we used the adsorption of pyridine to probe a series of oxides containing Nb_2O_5 *on* and *in* SiO_2, systems which we refer to as *surface phase* and *mixed* oxides, respectively. The objective was to relate the acidic properties of these samples to the structural characteristics of Nb_2O_5 in different environments.

METHODS

Sample Preparation

The preparations of bulk Nb_2O_5 (*13*) and Nb_2O_5–SiO_2 surface phase oxides (*14*) have been described previously. Briefly, Nb_2O_5 was obtained from adding ammonium hydroxide to a methanol solution of niobium chloride and calcining the resulting precipitate after repeated washings. Nb_2O_5–SiO_2 was prepared by impregnating SiO_2 (Davison 952) with a hexane solution of niobium ethoxide to incipient wetness. The sample was then heated in flowing nitrogen at 673 K for 2 h and in flowing oxygen at 773 K for 2 h, which was the standard calcination procedure for all the oxides in this study.

Nb_2O_5/SiO_2 mixed oxides were prepared by coprecipitation. The procedure involved titrating a methanol solution of silicon chloride and niobium chloride with ammonium hydroxide to a pH of 7. The resulting precipitate was filtered and washed repeatedly until no chloride was detected by adding silver nitrate to the filtrate. The precipitate was then dried overnight at 373 K in stagnant air and treated with the standard calcination procedure.

Table 1 summarizes the list of samples and introduces the notations to be used in the following sections.

Physical Characterization

BET surface areas of the samples were measured with a commercial Quantasorb unit (Quantachrome Corp.). Powder X-ray diffraction (XRD) patterns were obtained with a Rigaku D/Max diffractometer using a Mo or Cu source.

Diffuse reflectance infrared spectroscopy (DRIFT) was used to examine the surface phase oxides. Spectra were obtained with an IBM 98 Fourier transform infrared (FTIR) spectrometer equipped with an IBM DRIFT accessory (A6106640).

Acidity Measurements

The adsorption of pyridine was used to (i) measure the heat of adsorption and (ii) to characterize the distribution of acid sites. We followed the thermogravimetric (TG) technique of Deeba and Hall (*15*) and used a Cahn 113 microbalance to measure the weight of adsorbed pyridine as a function of sample temperature and pyridine pressure. In a typical run the system was first purged of residue pyridine by heating and evacuat-

TABLE 1

Summary of Samples

Notation	Description	Wt% Nb_2O_5	$\frac{\text{mol of Nb}}{\text{mol of Nb + mol of Si}}$ (%)	BET Surface area[a] m^2/g sample	X-ray diffraction[a] pattern
SiO_2	Davison 952	0	0	300	Amorphous
NS(0.25)	0.25 monolayer of Nb_2O_5 on SiO_2	9.1	4	340	Amorphous
NS(1)	1 monolayer of Nb_2O_5 on SiO_2	29.3	16	273	Amorphous
NS25	Mixed Nb_2O_5/SiO_2 with 25 wt% Nb_2O_5	25	13	480	Amorphous
NS85	Mixed Nb_2O_5/SiO_2 with 85 wt% Nb_2O_5	85	72	16	Amorphous
Nb_2O_5	Bulk Nb_2O_5	100	100	83	TT

[a] Obtained after the standard calcination treatment (773 K for 2 h in flowing oxygen).

ing to a base pressure of ca. 10^{-6} Torr. The oxide was then introduced into the sample pan and purged in He at 723 K prior to being exposed to a constant pressure of pyridine. The vapor pressure of pyridine was controlled by a constant temperature ethylene glycol/water bath and varied between 0.2 and 5 Torr. At each pyridine pressure, the sample was kept at a constant temperature until a constant weight was achieved, which corresponded to an equilibrium uptake at that temperature and pressure. Similar equilibrium uptakes were obtained at temperature intervals of 25 K from 373 to 723 K. The entire procedure was then repeated at 4–5 different pyridine pressures.

Blank runs were made without the sample to correct for temperature-buoyancy effects and any adsorption of pyridine on the sample pan. After converting the corrected weight of adsorbed pyridine into a coverage, in molecules/cm^2, equilibrium isobars were obtained by plotting the pyridine coverage versus reciprocal temperature. From this plot, the heat of adsorption at a given coverage can be calculated from the Clausius–Clapeyron equation

$$\left.\frac{\Delta H_{\text{ads}}}{R}\right|_{\sigma} = -\left[\frac{d \ln P}{d(1/T)}\right]_{\sigma},$$

where ΔH_{ads} = isosteric heat of adsorption
σ = pyridine coverage
P = pyridine pressure
T = absolute temperature
R = gas constant.

Infrared spectra of adsorbed pyridine were obtained with an IBM 98 FTIR spectrometer. The design of the IR cell and detailed experimental procedure can be found elsewhere (*16*). A typical experimental sequence involved exposing the sample to pyridine at room temperature and taking spectra after the sample had been evacuated at 373, 473, and 573 K. The ratio of Lewis to Brønsted acid sites was calculated from the integrated areas of the 1450 and 1490 cm^{-1} absorption peaks of pyridine by following the procedure of Basila and Kantner (*17*).

RESULTS

Physical Characteristics

The BET surface areas and XRD results of all the samples after the standard calcination treatment are shown in Table 1. On the basis of per gram SiO_2, the surface areas of NS(0.25) and NS(I) were 374 and 386 m^2/g, respectively. The increase in surface area due to the introduction of a Nb_2O_5 surface phase was consistent with the surface area of 377 m^2/g SiO_2 previously reported for NS(I) (*14*). The X-ray diffraction patterns for these two samples were also indistinguishable from that of the SiO_2 support alone, as would be expected for a highly dispersed Nb_2O_5 surface phase (*14*).

For the mixed oxides, the surface area appeared to decrease with increasing Nb_2O_5 concentration, even though the NS85 sample had a lower surface area than bulk Nb_2O_5. We have no explanation for the latter observation except to note that in our experience, the surface areas of samples containing Nb_2O_5 as the major component were very sensitive to the final calcination temperature. The presence of SiO_2 in the mixed oxides affected the crystallization behavior of Nb_2O_5, which also appeared to be the case under more severe heat treatments as shown by the results in Table 2.

DRIFT was used to characterize the surface phase oxides as the contribution of the supported Nb_2O_5 can be obtained from subtracting that of the SiO_2 support. Figure 1 shows the difference spectra thus obtained for NS(0.25) and NS(I). There are two major peaks at ca. 740 and 920 cm^{-1}. The 740 cm^{-1} peak can be assigned to Nb–O–Nb chain linkages (*19*) and the 920 cm^{-1} peak, to Nb=O double bonds (*20–22*). In going from NS(0.25) to NS(I), the intensities of both peaks increased but the ratio of the 920 to 740 cm^{-1} peaks decreased. In other words,

TABLE 2

Phases of Nb_2O_5 Identified by X-Ray Diffraction as a Function of Heat Treatment[a]

Heat treatment (temperature in K, time in h)	NS25	NS85	Nb_2O_5
(773,2)	A[b]	A	TT
(1073,2)	A	TT	T
(1273,-)[c]	TT_{vpc}[b]	TT	T
(1273,48)	TT_{vpc}	M + T	H

[a] The notation of Shafer *et al.* (*18*) is used to describe the many modifications of Nb_2O_5; TT and T, low-temperature forms; M, medium-temperature form; and H, high-temperature form.

[b] A = amorphous, vpc = very poorly crystalline.

[c] (1273,-) means the sample was ramped to 1273 K without being held at that temperature.

there were more Nb–O–Nb linkages relative to Nb=O bonds in NS(I).

Heats of Adsorption

Table 3 summarizes the heats of adsorption (ΔH_{ads}) data as a function of pyridine coverage. Results of SiO_2 are not included because SiO_2 was only weakly acidic, with a corresponding heat of adsorption of 14.1 ± 1.2 kcal/mol at coverages of 1–2.5 × 10^{13} molecules/cm^2. This value agrees very well with the 12.4 kcal/mol reported by Fowkes (*23*) for pyridine adsorption on silica.

Heats of adsorption at low coverages could not be obtained for samples of low surface areas (NS85, Nb_2O_5) as the absolute weight gains were too small to measure accurately. In general, the variation of ΔH_{ads} with coverage was within the experimental uncertainties. Thus we use only the average values to establish qualitative trends among the samples.

Relating the magnitude of ΔH_{ads} to the strength of acidity, we noted that Nb_2O_5 as a pure oxide was more acidic than SiO_2 with a ΔH_{ads} of 22 kcal/mol. Adding a small amount of SiO_2 to Nb_2O_5 did not change the ΔH_{ads} much, as shown by Fig. 2 which compares NS85 with Nb_2O_5. Adding a small amount of Nb_2O_5 to SiO_2, on the other hand, resulted in a ΔH_{ads} of 38 kcal/mol for the

TABLE 3

Heats of Adsorption as a Function of Pyridine Coverage

σ × 10^{13} molecules/cm^2	Heat of adsorption, kcal/mol				
	NS(0.25)	NS(I)	NS25	NS85	Nb_2O_5
2.0			42.4 ± 6.8		
2.5			42.3 ± 6.6		
3.0			37.0 ± 7.4		
3.3	34.4 ± 3.1		33.0 ± 6.6		
4.1	35.0 ± 3.7				
5.0	35.2 ± 3.7		33.8 ± 4.5		
6.0	37.5 ± 4.6	33.4 ± 3.0	37.6 ± 4.2		
7.4	37.9 ± 4.6	29.2 ± 2.0	38.8 ± 3.9		
9.0	38.9 ± 4.6	29.2 ± 1.5	42.1 ± 3.8		
10.0				29.9 ± 4.1	24.0 ± 6.2
11.0	37.4 ± 5.0	33.4 ± 2.0	40.5 ± 3.8	20.8 ± 4.1	23.7 ± 5.7
13.5	37.0 ± 4.8	34.5 ± 2.0	36.9 ± 4.7	22.4 ± 2.6	22.3 ± 5.8
14.9				22.4 ± 3.0	20.5 ± 5.5
16.4				19.7 ± 3.7	18.9 ± 5.2
Average (rounded to two significant figures)	37	32	38	23	22

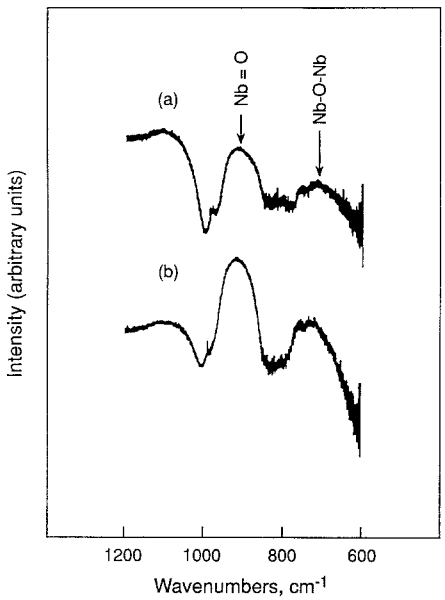

FIG. 1. DRIFT difference spectra for (a) NS(0.25) and (b) NS(I). Each curve was obtained by subtracting the spectrum of SiO_2 from that of the sample.

NS25 sample. This value was nearly identical to the 37 kcal/mol found for NS(0.25), making NS25 and NS(0.25) the two most acidic oxides in this series. The increase in Nb_2O_5 concentration from 0.25 to 1 monolayer in the surface phase oxides led to a ΔH_{ads} of 32 kcal/mol for NS(I). Finally, with the exception of NS85, all the composite oxides containing Nb_2O_5 had significantly higher heats of adsorption than bulk Nb_2O_5.

Distribution of Acid Sites

Table 4 summarizes the FTIR data of pyridine adsorbed on the oxides. Again, results for SiO_2 are not included since very little pyridine remained adsorbed at treatment temperatures above 373 K. The adsorption of pyridine on bulk Nb_2O_5 revealed both Lewis and Brønsted acid sites, with the former being more dominant. Furthermore, the ratio of Lewis to Brønsted acid sites (henceforth denoted as the L/B ratio) increased with increasing treatment temperature. This trend indicated that Brønsted acid sites were weaker than Lewis acid sites on Nb_2O_5 since pyridine desorbed from them preferentially.

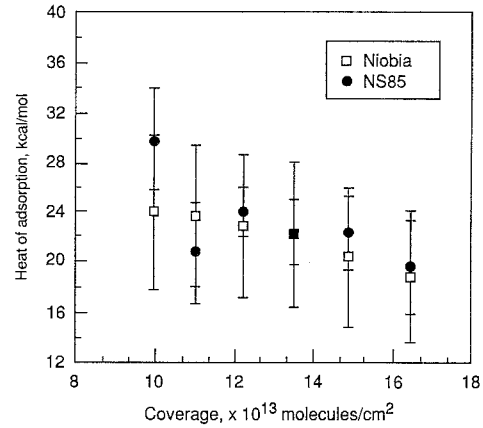

FIG. 2. Heats of adsorption as a function of pyridine coverage on Nb_2O_5 and NS85.

The FTIR spectra of NS85 were very noisy due to the low surface area of the sample and the peaks could not be resolved after a pretreatment temperature of 573 K. Still, the results at the lower pretreatment temperatures were similar to those of Nb_2O_5, consistent with the ΔH_{ads} data which suggested that these two samples had similar acid strengths. By comparison the NS25 sample had at 373 K a higher L/B ratio, which also increased with increasing treatment temperature.

The NS(0.25) sample was unique in that the L/B ratio remained roughly constant with thermal treatment, suggesting that this sample possessed strong Brønsted acid

TABLE 4

Summary of FTIR Results for Pyridine Adsorption

Sample	Ratio of Lewis to Brønsted acid sites		
	373 K[a]	473 K[a]	573 K[a]
NS(0.25)	8.5	8.0	7.0
NS(I)	7.4	15	19
NS25	8.1	16	21
NS85	4	9	—[b]
Nb_2O_5	3.8	7.1	20

[a] Temperature at which the sample was evacuated.
[b] Spectrum too noisy to resolve due to the small amount of pyridine adsorbed.

TABLE 5

Acidic Properties of Composite Oxides Containing Niobia

Sample	Experimental findings
NS(0.25)	Strong Lewis and Brønsted acid sites
NS(I)	Moderately strong Lewis acid sites, weak Brønsted acid sites
NS25	Strong Lewis acid sites, weak Brønsted acid sites
NS85	Little additional acidity beyond bulk Nb_2O_5

sites. These sites were apparently absent when the Nb_2O_5 surface phase concentration approached a monolayer, as the L/B ratio of NS(I) indicated a preferential desorption from Brønsted acid sites at high treatment temperatures.

DISCUSSION

The surface acidity of solids is critically dependent on the method of measurement as well as the pretreatment used in a particular method (*24, 25*). In this study the same set of procedures was consistently applied to all oxides so that a meaningful comparison can be made among them. As shown in Table 5, with the exception of NS85, all the composite oxides containing SiO_2 and Nb_2O_5 possessed stronger acid sites than either of the pure components. Although this observation is hardly surprising, our experimental findings deviated from what current models of acidity would predict. For example, the model of Kataoka and Dumesic (*4*) predicts no Brønsted acidity for NS(0.25) and the model of Tanabe (*1*) predicts no Lewis acidity for NS25. One reason for these discrepancies could be that the structures assumed in these models do not correspond to what actually existed in our samples. Our discussion must then turn to the structural characteristics of these composite oxides.

Lately there have been many studies on SiO_2-supported Nb_2O_5. Even though these studies differed somewhat in the support and precursor used and the experimental technique, they have led to a clearer picture on the structure of the surface phase Nb_2O_5. Using extended X-ray absorption fine structure (EXAFS), Yoshida *et al.* (*26*) concluded that at low loadings, the surface phase Nb_2O_5 exists as a tetrahedral species with a Nb=O double bond. For Nb_2O_5 monomers supported on SiO_2, Nishimura *et al.* (*8*) found a Raman band at 880 cm^{-1} which is close to the 850 cm^{-1} band for tetrahedral $YNbO_4$. They also proposed a structural model containing Nb=O bonds. Jehng and Wachs (*27*) noted that a tetrahedral NbO_4 structure should be rare because the Nb cation is too large to fit into an oxygen–anion tetrahedron. But such a size constraint might not be critical for a surface species since the oxygen anions are not necessarily close-packed. Their own laser Raman spectroscopy (LRS) data for a 2% SiO_2-supported Nb_2O_5 sample were inconclusive because the signal in the region of interest overlapped with that of the support (*28*).

We propose the structure shown in Fig. 3a to be the basic building block in our NS(0.25) sample. Other than the experimental evidence cited above, the quantum chemical calculations of Kobayashi *et al.* (*29*) also showed this to be a stable structure. Furthermore, the charge on the Nb

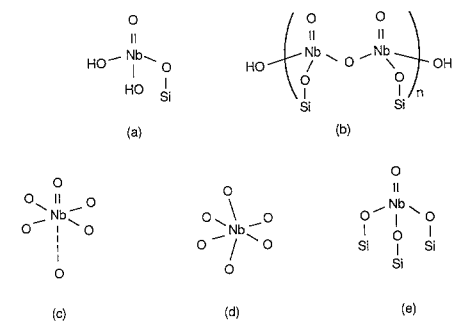

FIG. 3. Proposed structural models of niobia in the composite oxides: (a) monomeric tetrahedral species, (b) polymeric tetrahedral species, (c) highly distorted octahedral species (Ref. (*28*)), (d) slightly distorted octahedral species (Ref. (*28*)), and (e) tetrahedral species in NS25.

atom was calculated to be +1.54, making it a potential Lewis site. The two hydroxyl groups in this structure can function as Brønsted acid sites. In fact, strong Brønsted acidity is expected because upon proton removal, charge delocalization can occur onto the terminal oxygen atom and into the support through the Nb–O–Si bond (*30*). Our DRIFT data showed both Nb=O bonds and Nb–O–Nb linkages, suggesting the linking of these basic building blocks to form polymeric species as shown in Fig. 3b. Such a structure would also be consistent with the observed L/B ratio as there are less terminal OH groups to act as Brønsted acid sites.

At high loadings of surface phase Nb_2O_5, Yoshida *et al.* (*26*) reported square-pyramidal species in an aggregated state. Figure 3c represents such a structure, which is also referred to as a highly distorted octahedron by Jehng and Wachs (*27*). Jehng and Wachs (*28*) also found that Nb_2O_5 aggregates on SiO_2 at a concentration above 2% into what is likely to be a slightly distorted octahedron as shown in Fig. 3d. We thus believe these two structures to be the basic building blocks in our NS(I) sample. With increasing Nb_2O_5 concentration, the shift from tetrahedral to octahedral Nb as the dominant species could account for the lower heat of adsorption and weaker Brønsted acid sites for NS(I). Since one of the structures does not contain a Nb=O bond, the Nb=O absorption peak was found not to scale with Nb_2O_5 coverage in DRIFT. Furthermore, the relative dominance of the Nb–O–Nb absorption peak suggests extensive linkings of these octahedrons in this sample.

Jehng and Wachs (*27*) postulated that highly distorted NbO_6 octahedron gives rise to Lewis acid and slightly distorted NbO_6 octahedron, to Brønsted acid. A combination of these structures would then result in a distribution of acid sites. Our FTIR data showed that NS(I) possessed stronger Lewis than Brønsted acidity due presumably to the Nb=O bond in the highly distorted octahedron. In a sample similar to our NS(I), Shirai *et al.* (*10*) found that pyridine desorbed from Brønsted acid sites but not from Lewis acid sites when the sample was evacuated from 473 to 773 K. This trend is totally consistent with ours, even though these authors did not include Nb=O bonds in their structural model.

Structural data for Nb_2O_5/SiO_2 mixed oxides are scarce. The Raman spectrum for NS25 (*16*) consisted of a broad peak which could be assigned to a combination of tetrahedral and highly distorted octahedral species. Since the heat of adsorption was high and similar in magnitude to that on NS(0.25), we proposed the dominant structure in NS25 to be a tetrahedral species as shown in Fig. 3e. This structure differed from that of NS(0.25) in not having terminal OH groups. The bonding to Si instead explained the lack of strong Brønsted acid sites.

Apparently the tetrahedral species was stabilized in NS25 by its interaction with SiO_2 as in the case of the surface phase oxide. Recall, however, that heating this sample to 1273 K resulted in the incipient crystallization of TT–Nb_2O_5 (see Table 2). Since the crystallization process involved the aggregation of niobia, one would expect a conversion from tetrahedral to octahedral species, similar to the structural evolution of the surface phase oxide with increasing niobia concentration. To test this hypothesis, ΔH_{ads} data were obtained for a NS25 sample heat treated to 1273 K. The average ΔH_{ads} turned out to be 32 kcal/mol (*16*), which was significantly lower than that of the untreated sample. The fact that this value is identical to that of NS(I) might be a coincidence, but the main observation remains that a decrease in acid strength accompanied the tetrahedral to octahedral conversion in both oxides.

Niobia obviously interacted with silica in NS85, as it did not crystallize into TT–Nb_2O_5 as the pure oxide under the same treatment. Thus, the lack of additional acidity beyond Nb_2O_5 in the NS85 sample appeared to contradict with predictive models (*1, 2*). However, the predictive models start

by assuming a particular structure. Kung (*2*) assumed that a substituting cation will occupy a lattice position in the host oxide, whereas Tanabe (*1*) assumed that a substituting cation maintain locally its own bulk coordination but the surrounding oxygen anions maintain the coordination of the host oxide. In the case of SiO_2, its rigid tetrahedral structure due to strong Si–O covalent bonds could perhaps be fitted into a less rigid Nb_2O_5 framework without causing much perturbations. Any contribution to acidity would then likely come from Nb–O–Si linkages at the interface. Due to the low surface area of the NS85 sample, this or similar subtle differences in acidity could just not be detected by our experimental techniques.

SUMMARY

Based on the results of pyridine adsorption and literature data, we have established the acidity-structure relationship of a series of composite containing niobia. Niobia as a tetrahedral species with a Nb=O bond, stabilized by its interaction with silica, shows strong Lewis acidity. This species also has strong Brønsted acidity if it contains terminal hydroxyl groups, as in the case of silica-supported niobia.

Octahedral niobia becomes dominant with increasing niobia concentration and/or heat treatment temperature. The highly distorted octahedral species, also with a Nb=O bond, gives moderately strong Lewis acidity whereas the slightly distorted octahedral species gives weak Brønsted acidity.

Niobia–silica interactions, which are believed to stabilize the tetrahedral and highly distorted octahedral species, thus lead to enhanced acidity in the composite oxides over the pure oxides. When niobia is the major component, however, the addition of silica does not change the acidic properties significantly because very little perturbations are introduced into the host matrix.

ACKNOWLEDGMENT

This research was supported in part by the Niobium Products Company, Inc.

REFERENCES

1. Tanabe, K., *in* "Catalysis Science and Technology" (J. R. Anderson and M. Boudart, Eds.), Vol. 2, p. 231. Springer-Verlag, Berlin, 1981.
2. Kung, H. H., *J. Solid State Chem.* **52,** 191 (1984).
3. Connell, G., and Dumesic, J. A., *J. Catal.* **105,** 285 (1987).
4. Kataoka, T., and Dumesic, J. A., *J. Catal.* **112,** 66 (1988).
5. Weissman, J. G., Ko, E. I., and Wynblatt, P., *J. Catal.* **125,** 9 (1990).
6. Iizuka, T., Ogasawara, K., and Tanabe, K., *Bull. Chem. Soc., Jpn.* **56,** 2927 (1983).
7. Chen, Z., Izuka, T., and Tanabe, K., *Chem. Lett.,* 1085 (1984).
8. Nishimura, M., Asakura, K., and Iwasawa, Y., *J. Chem. Soc., Chem. Commun.* 1660 (1986).
9. Asakura, K., and Iwasawa, Y., *Chem. Lett.,* 859 (1986).
10. Shirai, M., Ichikuni, N., Asakura, K., and Iwasawa, Y., *Catalysis Today,* **8**(1), 57 (1990).
11. Datka, J., Turek, A., Jehng, J. M., and Wachs, I. E., submitted for publication.
12. Okazaki, S., and Okuyama, T., *Bull. Chem. Soc. Jpn.* **56,** 2159 (1983).
13. Ko, E. I., Hupp, J. M., Rogan, F. H., and Wagner, N. J., *J. Catal.* **84,** 85 (1983).
14. Ko, E. I., Bafrali, R., Nuhfer, N. T., and Wagner, N. J., *J. Catal.* **95,** 260 (1985).
15. Deeba, M., and Hall, W. K., *Z. Phys. Chem.* **144,** 85 (1985).
16. Burke, P. A., Ph.D. thesis, Carnegie Mellon University, 1989.
17. Basila, M. R., and Kantner, T., *J. Phys. Chem.* **70,** 1681 (1966).
18. Shafer, H., Gruehn, R., and Schulte, F., *Angew. Chem. Int. Ed. Eng.* **5,** 40 (1966).
19. Prashar, P., and Tandon, J. P., *Z. Naturf.* **256,** 32 (1970).
20. Griffith, W. P., and Wickins, T. D., *J. Chem. Soc. A,* 675 (1967).
21. Djordjevec, C., and Katovic, V., *J. Chem. Soc. A,* 3382 (1970).
22. Katovic, V., and Djordjevec, C., *Inorg. Chem.* **9,** 1720 (1970).
23. Fowkes, F. M., *Polym. Mater. Sci. Eng.* **53,** 560 (1985).
24. Tanabe, K., "Solid Acids and Bases." Academic Press, New York, 1970.
25. Benesi, H. A., and Winquist, B. H. C., *in* "Advances in Catalysis" (D. D. Eley, H. Pines, and P. B. Weisz, Eds.), Vol. 27, p. 97. Academic Press, New York, 1978.

26. Yoshida, S., Nishimura, Y., Tanaka, T., Kanai, H., and Funabiki, T., *Catalysis Today,* **8**(1), 67 (1990).
27. Jehng, J.-M., and Wachs, I. E., submitted for publication.
28. Jehng, J.-M. and Wachs, I. E., *Catalysis Today,* **8**(1), 37 (1990).
29. Kobayashi, H., Yamaguchi, M., Tanaka, T., Nishimura, Y., Kawami, H., and Yoshida, S., *J. Phys. Chem.* **92,** 2516 (1988).
30. Bernholc, J., Horsley, J. A., Murrell, L. L., Sherman, L. G., and Soled, S., *J. Phys. Chem.* **91,** 1526 (1987).